Available online at www.sciencedirect.com
SCIENCE DIRECT®
Journal of Catalysis 221 (2004) 541–548
JOURNAL OF CATALYSIS
www.elsevier.com/locate/jcat

Intrinsic kinetics of thiophene hydrodesulfurization on a sulfided $NiMo/SiO_2$ planar model catalyst

A. Borgna, E.J.M. Hensen, J.A.R. van Veen, and J.W. Niemantsverdriet *

Schuit Institute of Catalysis, Eindhoven University of Technology, PO Box 513, 5600 MB Eindhoven, The Netherlands

Received 30 June 2003; revised 1 September 2003; accepted 10 September 2003

Abstract

The kinetics of thiophene hydrodesulfurization is studied on a planar surface science model of a sulfided $NiMo/SiO_2$ catalyst under diffusion-limitation-free conditions in a batch reactor at atmospheric pressure and temperatures between 575 and 675 K. A Langmuir–Hinshelwood model is used to analyze the data and to derive activation energies and heats of adsorption for thiophene and hydrogen sulfide. The work illustrates the feasibility of kinetic and mechanistic studies using planar models of catalysts which can be prepared and manipulated with procedures available in surface science.

Keywords: Planar model catalysts; Hydrodesulfurization; Intrinsic kinetics; $NiMo/SiO_2$ catalyst

1. Introduction

Hydrodesulfurization (HDS) is one of the largest processes in petroleum refining, and the key tool for producing clean transportation fuels. In recent years, HDS has gained importance due to more stringent legislation for vehicular emissions and fuel quality and an increasing need to process low-quality oil feedstocks, which contain larger amounts of sulfur compounds. While the structure of HDS catalysts, usually CoMo or NiMo mixed sulfides supported on high surface area carriers like γ-Al_2O_3 and SiO_2–Al_2O_3, has been studied in great detail [1–3], essential aspects of the HDS reaction mechanism and kinetics are not fully elucidated yet. Most studies on HDS kinetics were performed using model sulfur compounds such as thiophene, benzothiophene, and dibenzothiophene, which are better representative for sulfur compounds in oil feedstocks than aliphatic thiols. Even for thiophene hydrodesulfurization, which has been widely studied as one of the simplest HDS reactions, the kinetics and the reaction mechanism are still under debate. For instance, both the direct C–S bond cleavage [4,5] and the "hydrogenation" pathway, in which the hydrogenation of one or both C=C double bonds takes place before the C–S cleavage [2,6], have been proposed for thiophene HDS.

To understand the mechanism and to validate theoretical studies [7–11], there is a clear need to determine intrinsic kinetic parameters such as activation energies over a temperature range that is as broad as possible [12]. Also, it is imperative to determine heats of adsorption of the participating species as accurately as possible because these values may enter the apparent activation energy.

Model catalysts, consisting of a planar conducting substrate with a thin oxide layer on top of which the active phase was deposited, have been successfully applied in catalysis research [13]. One of the most important advantages of these systems derives from the fact that the full potential of surface science techniques can be used to obtain a detailed structural characterization of the active phase. In previous papers [14–17], we have shown that these planar model systems can be successfully applied to obtain more insight in the formation of the active phases in CoMo–, NiMo–, CoW– and NiW–sulfide catalysts.

Another important advantage of planar model catalysts is the absence of pores, excluding internal mass transfer limitations on the chemical kinetics. Thus, catalytic measurements can be performed under essentially diffusion-limitation-free conditions. In addition, the absence of pores might also facilitate detection of reaction intermediates, thereby increasing the probability of identifying them. Hence, planar model catalysts may become an important tool for obtaining an

* Corresponding author.
E-mail address: j.w.niemantsverdriet@tue.nl (J.W. Niemantsverdriet).

0021-9517/$ – see front matter
doi:10.1016/j.jcat.2003.09.018

increased knowledge on structure-activity relationships for HDS catalysts.

The purpose of this paper is to demonstrate that intrinsic kinetic parameters such as activation energies and heats of adsorption can be determined with reasonable accuracy for thiophene hydrodesulfurization on a planar sulfided $NiMo/SiO_2$ model catalyst.

2. Experimental

$NiMo/SiO_2$ planar model catalysts consisting of a Si(100) wafer covered by a thin layer of SiO_2 as support were prepared by spin coating as previously described [14–17]. A Si(100) single-crystal wafer was oxidized in air at 1023 K for 24 h. After calcination the wafers were cleaned in a H_2O_2/NH_4OH (3/2 v/v) solution at 338 K and then the surface was hydroxylated in boiling water for 20–30 min. Subsequently, these model supports were spin-coated in nitrogen atmosphere at 2800 rpm with an aqueous solution containing $Ni(NO_3)_2 \cdot 6H_2O$ (Merck, p.a.) and $(NH_4)_6Mo_7O_{24} \cdot 4H_2O$ (Merck, purity > 97%) with an atomic ratio of 1:3, respectively. The concentration of the precursor solution was adjusted to result in the required metal loadings (2 Ni at./nm^2 and 6 Mo at./nm^2).

Thiophene HDS activity measurements were carried out at atmospheric pressure in thiophene (Acros, purity > 99%)/hydrogen (Hoekloos, purity > 99.99%) mixtures, using He (Hoekloos, purity 99.95%) as balance. The catalysts were presulfided in a flow (60 ml/min) of a mixture of 10 vol% H_2S in H_2 (Scott Chemicals) by heating at a rate of 5 K/min to the desired sulfidation temperature and keeping the sample at this temperature for 1 h. The catalyst temperature was then adjusted to the desired reaction temperature. Subsequently, the reactor was flushed with the reactant mixture for 5 min at the reaction temperature. The reaction was then carried out in batch mode by closing the reactor inlet and outlet. This was marked as zero reaction time. After a reaction time of 1 h a gas-phase sample was taken from the reactor using a precision sampling gas syringe which was injected on a DB-1 column to analyze the following main products: C1–C3 hydrocarbons, 1-butene, *n*-butane, *trans*-2-butene, *cis*-2-butene, and thiophene. The HDS activities are expressed as thiophene conversion after 1 h of reaction time and per 5 cm^2 of model catalyst. These values were corrected for blank thiophene conversion measured using an empty reactor. A next experiment was performed after the catalyst was resulfided at 673 K for 1 h. The partial pressure of H_2 was varied between 40 and 96 vol% (4 vol% thiophene, He as balance) and the partial pressure of thiophene between 1 and 8 vol% (90 vol% H_2, He as balance). In addition, the H_2S partial pressure was varied from 0 to 5.6 vol% (4 vol% thiophene, 90 vol% H_2, He as balance).

3. Results

The catalytic measurements were carried out over a temperature range between 573 and 673 K, with a resulfidation step performed between each experiment. This procedure allows reproducible and reliable kinetic data to be obtained, by excluding effects due to deactivation [18]. The main reaction products observed during thiophene conversion were regular HDS products: 1-butene, *cis*- and *trans*-2-butene, and a small amount of cracking compounds. Only traces of tetrahydrothiophene and dihydrothiophenes were detected.

Fig. 1 shows double-log plots of the kinetic data at different temperatures measured varying the partial pressures of hydrogen, thiophene, and H_2S, respectively. Linear fits, used to determine the reaction orders, are also displayed in this figure. All reaction orders have been collected in Tables 1–3. At all temperatures we observe positive orders in thiophene and hydrogen and moderately negative orders in H_2S. Moreover, while the reaction order in thiophene is strongly de-

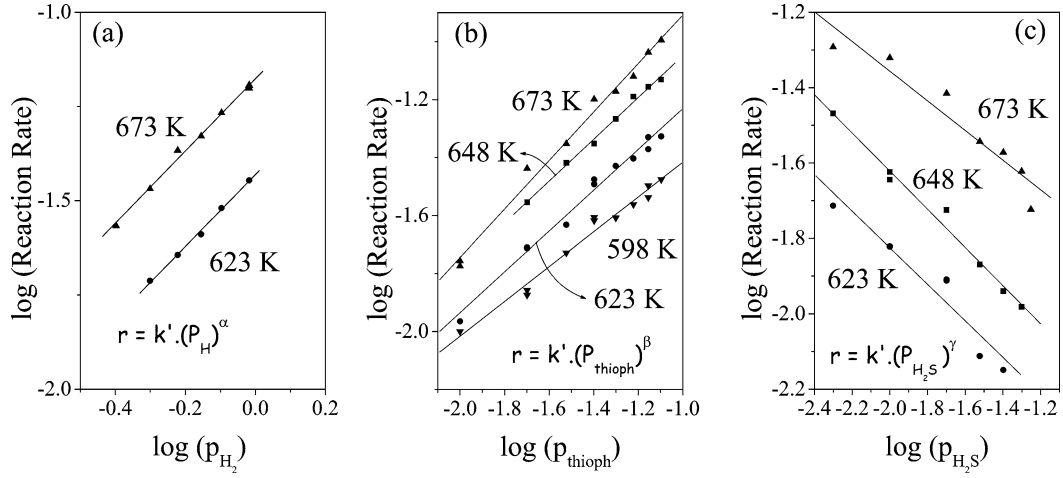

Fig. 1. Double-log plot of the dependence of the rate of thiophene HDS on the partial pressures of hydrogen, thiophene, and H_2S at different temperatures. (a) Influence of hydrogen, $p_{thioph} = 4$ vol% and $p_{H_2S} = 0$ vol%; (b) influence of thiophene, $p_{H_2} = 90$ vol% and $p_{H_2S} = 0$ vol%; (c) influence of H_2S, $p_{thioph} = 4$ vol% and $p_{H_2} = 90$ vol%.

Table 1
Reaction orders in hydrogen and hydrogen adsorption constants

Temperature (K)	Power-rate law, reaction order	L–H model, adsorption constant (bar^{-1})
623	0.95 ± 0.02	0.0020 ± 0.003
673	0.94 ± 0.03	0.0043 ± 0.004

Table 2
Reaction orders in thiophene, thiophene adsorption constants, and estimated coverages of thiophene

Temperature (K)	Power-rate law, reaction order (n_T)	L–H model		
		Adsorption constant (bar^{-1})	θ_{thioph}	$n_T = (1-\theta_{thioph})$
598	0.58 ± 0.03	11.9 ± 1.4	0.42	0.58
623	0.65 ± 0.03	9.1 ± 1.1	0.35	0.65
648	0.71 ± 0.03	5.6 ± 0.8	0.25	0.75
673	0.80 ± 0.03	3.5 ± 0.7	0.17	0.83

Table 3
Reaction orders in H_2S and H_2S adsorption constants

Temperature (K)	Power-rate law, reaction order	L–H model, adsorption constant[a]
623	-0.43 ± 0.06	107.2 ± 10.1
648	-0.50 ± 0.03	68.7 ± 5.0
673	-0.35 ± 0.05	28.9 ± 2.1

[a] Dimensionless.

pendent on the temperature, the variation of the hydrogen reaction order is much less and it remains close to unity as a function of reaction temperature. The lower reaction order of thiophene as compared to the reaction order in hydrogen clearly indicates that thiophene adsorbs much stronger than hydrogen. This is consistent with the larger change in reaction order as a function of temperature. The negative order in H_2S indicates that the HDS reaction is inhibited by H_2S, which is in agreement with the general notion of competition of hydrogen sulfide and sulfur-containing organics for sulfur-defect sites.

The trends in the reaction orders are in agreement with the literature [19,20]. For instance, Leliveld et al. [20] found reaction orders in H_2, thiophene, and H_2S of 1.2, 0.7, and -0.6, respectively, for a $CoMo/Al_2O_3$ catalyst at 673 K.

Heats of adsorption and activation energies can be derived once a kinetic model has been adopted. Several mechanisms and associated kinetic models for the hydrodesulfurization of thiophene have been proposed in the literature [6,21–30]. Although the precise mechanism of thiophene HDS is still under debate, we assume an often-used simplified reaction network consisting of steps, in which thiophene (T) and hydrogen sulfide (H_2S) exclusively adsorb on sulfur vacancies, denoted by Δ, and hydrogen (H_2) adsorbs dissociatively on equivalent sites different from those where thiophene and hydrogen sulfide adsorb (indicated by $*$).

$$T + \Delta \overset{K_T}{\longleftrightarrow} T\Delta,$$

$$H_2 + 2* \overset{K_{H_2}}{\longleftrightarrow} 2H*,$$

$$T\Delta + 2H* \overset{k}{\rightarrow} B + S\Delta + 2*,$$

$$S\Delta + H_2 \overset{K_{H_2S}^{-1}}{\longleftrightarrow} H_2S + \Delta.$$

In this mechanism, butadiene (B) reacts further to butenes and butane in kinetically insignificant steps [24]. We assume that the surface reaction between adsorbed thiophene and H_2 is the rate-limiting step and that H_2S adsorption takes place on sulfur vacancies exclusively, in competition with thiophene adsorption. Using quantum-mechanical calculations, Neurock and Van Santen [10] suggested that either the carbon–sulfur bond cleavage surface reaction or the hydrogenative sulfur removal reaction that creates sulfur vacancies can be considered as rate-limiting step for thiophene HDS. Furthermore, a reaction order in thiophene between 0 and 1 also indicates that the surface reaction involving thiophene is likely to be the rate-determining step [6]. The above mechanism leads to the following Langmuir–Hinshelwood rate expression:

$$r = \frac{k K_T K_{H_2} p_T p_{H_2}}{(1 + K_T p_T + K_{H_2S} p_{H_2S}/p_{H_2})(1 + K_{H_2}^{1/2} p_{H_2}^{1/2})^2}, \quad (1)$$

where k is the rate constant of the rate-determining step and K_T, K_{H_2}, K_{H_2S} are the adsorption constants of thiophene, H_2 and H_2S, respectively. Since the catalytic data were obtained at very low thiophene conversion (usually lower than 1.5–2%), the inhibiting effect of H_2S can be neglected in measurements performed without adding H_2S. In this case the rate simplifies to

$$r = \frac{k K_T K_{H_2} p_T p_{H_2}}{(1 + K_T p_T)(1 + K_{H_2}^{1/2} p_{H_2}^{1/2})^2}. \quad (2)$$

For measurements at constant thiophene partial pressure and variable H_2 partial pressure, the reaction rate equation can be further simplified as

$$r = \frac{k' K_{H_2} p_{H_2}}{(1 + K_{H_2}^{1/2} p_{H_2}^{1/2})^2}, \quad (3)$$

where

$$k' = \frac{k K_T p_T}{(1 + K_T p_T)}. \quad (4)$$

Fig. 2 shows that the experimental data are satisfactorily described using the L–H equation derived from the reaction mechanism, giving an estimation of the adsorption equilibrium constants of hydrogen at various temperatures. The optimized value for the adsorption equilibrium constant of hydrogen at 673 K is $0.0043 \pm 0.004\ bar^{-1}$, indicating that the adsorption equilibrium constant is statistically nondifferent from zero. Hence the term $(1 + K_{H_2}^{1/2} p_{H_2}^{1/2})^2$ may be safely assumed to equal unity. It is important to note that this is in good agreement with the order in H_2 equaling 0.94, i.e., close to one. In a similar manner, the adsorption equilibrium constants of thiophene and H_2S are obtained from L–H

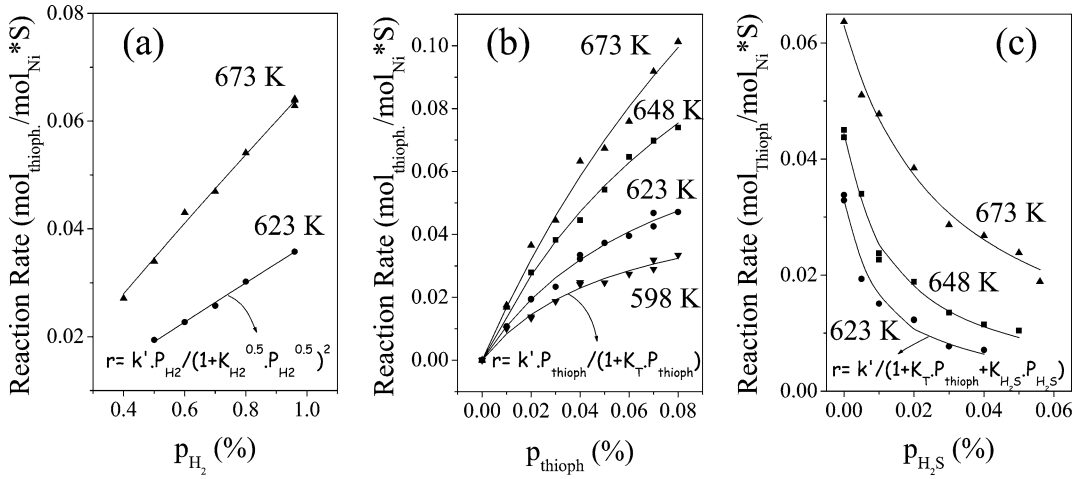

Fig. 2. Dependence of the rate of thiophene hydrodesulfurization on the partial pressures of hydrogen, thiophene, and H_2S at different temperatures, along with data fit according to the Langmuir–Hinshelwood kinetic model. (a) Influence of hydrogen, $p_{\text{thioph}} = 4$ vol% and $p_{H_2S} = 0$ vol%; (b) influence of thiophene, $p_{H_2} = 90$ vol% and $p_{H_2S} = 0$ vol%; (c) influence of H_2S, $p_{\text{thioph}} = 4$ vol% and $p_{H_2} = 90$ vol%.

fitting. Fig. 2 shows the quality of the fits. The optimized values for the adsorption equilibrium constants at 673 K of thiophene and H_2S are 3.5 ± 0.7 bar^{-1} and 28.9 ± 1.8, respectively. The values of the equilibrium constants reflect a relatively strong adsorption of thiophene and in particular of H_2S. By measuring the reaction rate constant and the adsorption equilibrium constants at different temperatures, the intrinsic kinetic parameters, the activation energy ($E_{\text{act}}^{\text{rds}}$), and the heat of adsorptions (ΔH_{ads}), can be obtained.

3.1. Reaction kinetics at different temperatures

Fig. 1a shows two nearly parallel straight lines when measurements are performed at different temperatures varying the hydrogen partial pressure. This plot clearly indicates that there is no significant change in the reaction order in hydrogen in the analyzed temperature range. Furthermore, the fitting of the catalytic data obtained at 635 K using the L–H kinetic model leads to a hydrogen adsorption constant that is statistically not different from zero. Therefore, we conclude that the hydrogen is only weakly adsorbed on the catalyst surface and hence the respective terms in the denominators of (2) and (3) can be ignored. On the contrary, the reaction order in thiophene decreases significantly with a decrease in temperature. For instance, the reaction order in thiophene varies from 0.8 to 0.65 when the reaction temperature decreases from 673 to 623 K. All kinetic data were satisfactorily fitted using both power-law equations and L–H kinetic models. Table 2 summarizes the kinetic parameters, reaction orders in thiophene and thiophene adsorption constants. The expected evolutions of the kinetic parameters, i.e., a decrease of the reaction order in thiophene and an increase of the equilibrium constant as a function of reaction temperature, are observed. Furthermore, the adsorption equilibrium constants allow for the estimation of thiophene H_2S coverages through

$$\theta_{\text{thioph}} = \frac{K_{\text{T}} p_{\text{T}}}{(1 + K_{\text{T}} p_{\text{T}} + K_{H_2S} p_{H_2S}/p_{H_2})} \tag{5}$$

and

$$\theta_{H_2S} = \frac{K_{H_2S} p_{H_2S}}{(1 + K_{\text{T}} p_{\text{T}} + K_{H_2S} p_{H_2S}/p_{H_2})}. \tag{6}$$

At very low thiophene conversion, $\theta_{H_2S} \to 0$ and Eq. (5) simplifies to

$$\theta_{\text{thioph}} = \frac{K_{\text{T}} p_{\text{T}}}{(1 + K_{\text{T}} p_{\text{T}})}. \tag{7}$$

The values of the estimated thiophene coverages computed from Eq. (7) are also included in Table 2. Applying the definition of reaction order, $n_i = (\partial \ln r / \partial \ln p_i)$ to the rate expression Eq. (1), one finds: $n_i = (1 - \theta_i)$. The values of $(1 - \theta_{\text{thioph}})$, also reported in Table 2, are indeed in good agreement with the values of the reaction orders determined by power-law fittings.

The apparent activation energy ($E_{\text{act}}^{\text{app}}$), derived from an Arrhenius plot, is 42 ± 2 kJ/mol, which is in rather good agreement with previous reported values for sulfided NiMo catalysts [18,29,31]. Similar values were also reported for sulfided CoMo [6,20,24,31] and MoS_2 [27] supported catalysts.

The intrinsic kinetic parameters, i.e., activation energy of the rate-determining step and heat of adsorption of thiophene, can be obtained by nonlinear multivariable regression of experimental data using the following reparameterized equation,

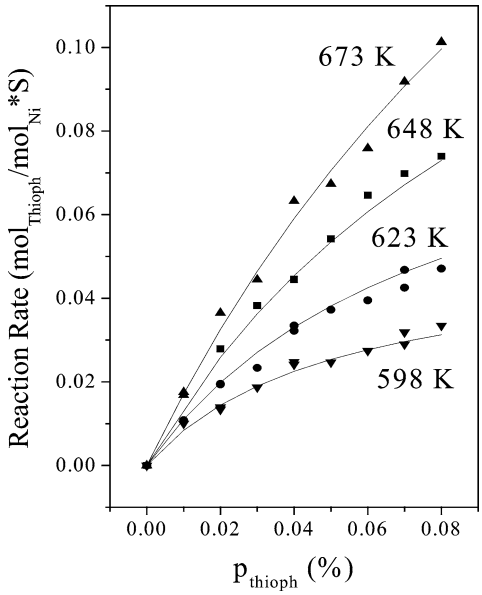

Fig. 3. Dependence of the rate of thiophene hydrodesulfurization on the partial pressures of thiophene at different temperatures, along with a nonlinear multivariable fitting according to the Langmuir–Hinshelwood model. $p_{H_2} = 90$ vol% and $p_{H_2S} = 0$ vol%.

Table 4
Intrinsic kinetic parameters measured on a $NiMo/SiO_2$ planar model catalyst without addition of H_2S

Parameter	Value	Standard error
k^0 ($mol_{thioph}/(mol_{Ni}\ S)$)	0.0998	0.0078
E_{act}^{rds} (kJ/mol)	83.3	7.3
K_{thioph}^0 at 623 K (bar^{-1})	8.3	1.1
$-\Delta H_{ads}^{thioph}$ (kJ/mol)	−57.8	10.9
χ^2	6.2×10^{-6}	–
R^2	0.99	–

$$r = k^0 \exp\left(-\frac{E_{act}^{rds}}{R}\left(\frac{1}{T} - \frac{1}{623}\right)\right) K_T^0 \times \exp\left(\frac{-\Delta H_{ads}^{thioph}}{R}\left(\frac{1}{T} - \frac{1}{623}\right)\right) p_T \Big/ \left(1 + K_T^0 \exp\left(\frac{-\Delta H_{ads}^{thioph}}{R}\left(\frac{1}{T} - \frac{1}{623}\right)\right) p_T\right), \quad (8)$$

where k^0 and K_T^0 are the reaction rate constant and the adsorption equilibrium constant of thiophene at 623 K, respectively. Fig. 3 shows that the experimental data are satisfactorily described by Eq. (8); the intrinsic kinetic parameters are summarized in Table 4. It is important to emphasize that the activation energy derived from L–H multivariable fittings is two times higher than the value obtained from a simple Arrhenius plot. The estimated values for the activation energy and for the heat of adsorption of thiophene are 83.3 ± 7.3 and -57.8 ± 10.9 kJ/mol, respectively.

Table 5
Intrinsic kinetic parameters measured on a $NiMo/SiO_2$ planar model catalyst with addition of H_2S

Parameter	Value	Standard error
k^0 ($mol_{thioph}/(mol_{Ni}\ S)$)	0.0967	0.0065
E_{act}^{rds} (kJ/mol)	83.5	1.8
K_{thioph}^0 at 623 K (bar^{-1})	8.7	1.0
$-\Delta H_{ads}^{thioph}$ (kJ/mol)	−57.8	10.9
$K_{H_2S}^0$ [a] at 623 K	138.9	19.6
$-\Delta H_{ads}^{H_2S}$ (kJ/mol)	−117.1	11.3
χ^2	6.4×10^{-6}	–
R^2	0.99	–

[a] Dimensionless.

When measurements are performed with addition of H_2S, the following L–H kinetic equation must be used:

$$r = \frac{k K_T p_T}{(1 + K_T p_T + K_{H_2S} p_{H_2S}/p_{H_2})}. \quad (9)$$

Similarly as above, the adsorption equilibrium constant of H_2S at different temperatures have been estimated; see Table 3. The comparison of these values with those corresponding to the thiophene adsorption indicates that H_2S adsorbs stronger than thiophene.

Finally, a nonlinear multivariable fitting can be applied to fit simultaneously all catalytic data obtained with and without H_2S addition. In this case, the following equation with six [6] fitting parameters must be used:

$$r = k^0 \exp\left(-\frac{E_{act}^{rds}}{R}\left(\frac{1}{T} - \frac{1}{623}\right)\right) K_T^0 \times \exp\left(\frac{-\Delta H_{ads}^{thioph}}{R}\left(\frac{1}{T} - \frac{1}{623}\right)\right) p_T \Big/ \left(1 + K_T^0 \exp\left(\frac{-\Delta H_{ads}^{thioph}}{R}\left(\frac{1}{T} - \frac{1}{623}\right)\right) p_T + K_{H_2S}^0 \exp\left(\frac{-\Delta H_{ads}^{H_2S}}{R}\left(\frac{1}{T} - \frac{1}{623}\right)\right)\right). \quad (10)$$

Table 5 summarizes the intrinsic kinetic parameters as well as the statistical parameters, χ^2 and R^2, showing the quality of the fits. Fig. 4 shows that the catalytic data obtained by varying the H_2S partial pressure are satisfactorily fitted with the above equation derived from a L–H model. It is important to emphasize that the intrinsic kinetic parameters corresponding to the thiophene adsorption, K_T^0 and ΔH_{ads}^{thioph}, and to the rate-limiting step of the reaction rate, k^0 and E_{act}^{rds}, are very close to those reported in Table 4 for the case that H_2S is nearly absent. The estimated value for the heat of adsorption of H_2S is -117.1 ± 11.3 kJ/mol.

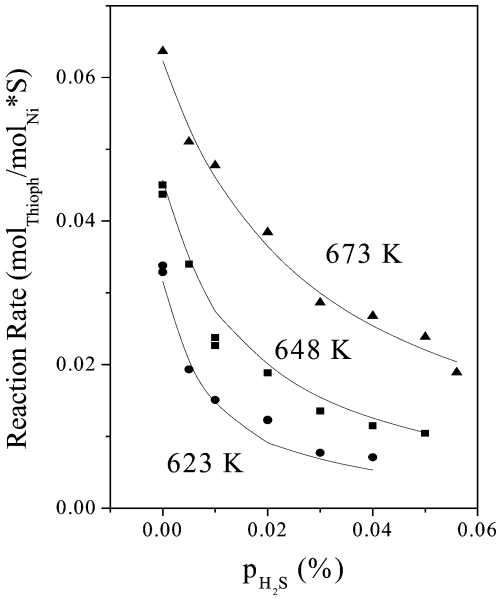

Fig. 4. Dependence of the rate of thiophene hydrodesulfurization on the partial pressures of H_2S at different temperatures, along with a nonlinear multivariable fitting according to the Langmuir–Hinshelwood model. $p_{H_2} = 90$ vol%, $p_{thioph} = 4$ vol%.

4. Discussion

The results reported here illustrate the feasibility of studying kinetics of thiophene hydrodesulfurization over a planar model catalyst of only 5 cm^2 total surface area in a batch reactor. An advantage of this approach is that the kinetics is not perturbed by diffusion limitations. It also opens the opportunity to study kinetics of reactions over catalysts that can be prepared and manipulated according to techniques from surface science and nanotechnology.

A kinetic model based on equilibrium adsorption of thiophene and H_2S on the same sites, equilibrium adsorption of H_2 on different sites, and a rate-determining surface reaction of thiophene with hydrogen to butadiene describes the data adequately. Corresponding intrinsic kinetic parameters are given in Tables 4 and 5.

The activation energy obtained from L–H fittings, $E_{act}^{rds} \approx 85$ kJ/mol, compares well with results of theoretical calculations by Neurock and van Santen for Ni_3S_2 clusters [10], which lead to overall reaction enthalpies for C–S scission and sulfur removal of 70 and 73 kJ/mol, respectively. Therefore, assuming that these overall reaction enthalpies represent a significant portion of the real activation barriers for these steps [10], a real activation energy of at least 70–75 kJ/mol should be obtained. Furthermore, these values are also in agreement with the activation energies reported by Ledoux et al. [32] for HDS on small metal sulfide clusters, ranging from 69 to 98 kJ/mol. It should be emphasized that the activation energies obtained from Arrhenius plots represent the apparent activation energy and not the real activation energy of the rate-determining step, i.e., E_{act}^{rds}. The relationship between the apparent and real activation energies can be derived from the reaction rate [18]:

$$E_{act}^{app} = E_{act}^{rds} + \left(1 - \Theta_T^{\#}\right) \cdot \Delta H_{ads}^{T} + \left(1 - \Theta_H^{*}\right) \cdot \Delta H_{ads}^{H_2} - \Theta_{H_2S}^{\#} \cdot \Delta H_{ads}^{H_2S}. \quad (11)$$

Two possibilities can be invoked to explain the apparent activation energy decreases as temperature increases. In a recent review [29], Startsev suggested that this behavior is most likely related to a change in the rate-limiting step in the HDS reaction mechanism. On the other hand, such a decrease of the apparent activation energy has been often attributed to a decrease of reactant surface coverage as temperature increases [6,18,33], according to Eq. (11). We stress here that the measurements reported in the present contribution are in line with this second hypothesis, i.e., the decrease in the activation energy is related to a coverage effect, which follows straightforwardly from the Langmuir–Hinshelwood model.

The adsorption equilibrium constants for both thiophene and H_2S have also been obtained from Langmuir–Hinshelwood fittings. Satterfield and Roberts [22] reported lower values for K_{H_2S} than for K_T between 508 and 538 K for $CoMo/Al_2O_3$, whereas the values of the adsorption equilibrium constants that can be derived from the data reported by Lee and Butt [24] strongly depend on the kinetic model. Ihm et al. [31] determined the adsorption equilibrium constants between 548 and 598 K of thiophene and H_2S over NiMo catalysts from both kinetic modeling and a chromatographic pulse technique. Interestingly, these authors have found that the adsorption equilibrium constant of H_2S is slightly higher than the one of thiophene from both methods.

In summary, the values of the kinetic parameters clearly indicate a relatively strong adsorption of thiophene and in particular H_2S, while hydrogen is very weakly adsorbed. The intrinsic kinetic parameters obtained by nonlinear multivariable fittings allow for the simulation of the evolution of the thiophene coverage and the apparent activation energy as a function of the temperature. The evolution of the apparent activation energy as a function of the temperature can be estimated as follows. If the hydrogen adsorption is neglected and the H_2S coverage is close to 0 due to the low thiophene conversion:

$$E_{act}^{app} \cong E_{act}^{rds} + (1 - \theta_{thioph}) \cdot \Delta H_{ads}^{T}. \quad (12)$$

Therefore, the intrinsic parameters reported in Table 4 allow for the simulation of θ_{thioph}, θ_{H_2S}, and E_{act}^{app}. The simulations are displayed in Fig. 5. It is clear that the H_2S coverage close to 0 under our experimental conditions and, therefore, Eq. (5) can safely be simplified to Eq. (7). Between 573 and 673 K, a relatively high thiophene surface coverage is obtained, leading to a decrease of the apparent activation energy from 60 to 35 kJ/mol. Thus, the average apparent activation energy in this temperature range is around 45 kJ/mol, which is in rather good agreement with the value derived from an Arrhenius plot. Once again, these results point out

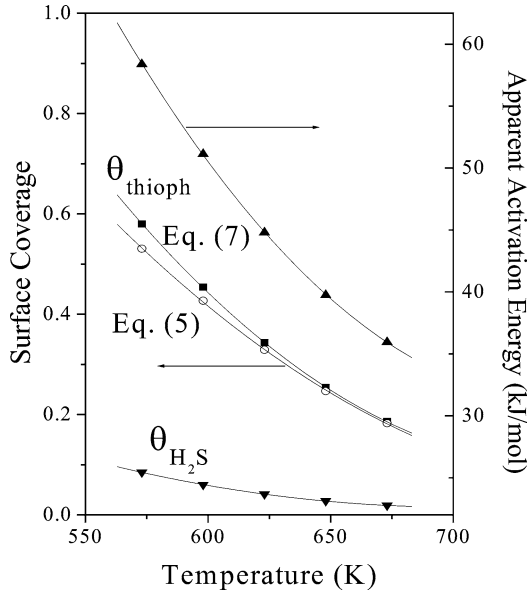

Fig. 5. Simulated evolution of the thiophene coverage and the apparent activation energy as a function of temperature, using the intrinsic parameters reported in Table 4.

that the decrease in the activation energy observed as the reaction temperature increases is most likely related to a coverage effect. Therefore, the true activation energy for the rate-limiting step for thiophene HDS, i.e., $E_{\text{act}}^{\text{rds}}$, would be around of 85 kJ/mol.

Obviously, at temperatures higher than 673 K, the thiophene coverage is very low ($\theta_{\text{thioph}} \to 0$) and, as a consequence, the apparent activation energy can be estimated by

$$E_{\text{act}}^{\text{app}} = E_{\text{act}}^{\text{rds}} + \Delta H_{\text{ads}}^{\text{T}}. \tag{13}$$

In this case, an apparent activation energy of about 25 kJ/mol can be obtained from our data. Once again we emphasize that this very low activation energy cannot be ascribed to diffusion limitations.

In a previous work [18], moderately negative apparent activation energies were reported at temperature higher than 673 K. From Eq. (12), it is clear that a negative apparent activation energy cannot be found because the adsorption energy of thiophene does not exceed the activation barrier. However, Eq. (12) was derived assuming that the rate-determining step does not involve hydrogen adsorption. However, if the surface reaction between adsorbed thiophene and adsorbed hydrogen is the rate-determining step, therefore the following expression for the apparent activation energy must be considered:

$$E_{\text{act}}^{\text{app}} = E_{\text{act}}^{\text{rds}} + \Delta H_{\text{ads}}^{\text{T}} + \Delta H_{\text{ads}}^{\text{H}_2}. \tag{14}$$

Although hydrogen adsorption under our experimental conditions was too weak to determine the corresponding heat of adsorption accurately, we will make use of values from molecular computations. Neurock and van Santen [10] reported values for the heat of adsorption of molecular hydrogen on Ni_3S_1 and Ni_3S_2 clusters in the range of -23–-62 kJ/mol. Typically, dissociative hydyrogen adsorption on a Ni_3S_2 clusters results in an energy change of 30 kJ/mol and represents one of the less favorable adsorption modes [10]. This value renders the apparent activation energy negative in line with the present experimental results. Our proposal for a surface reaction between adsorbed thiophene and hydrogen is thus in line with the present observations.

A broad range of values for the heats of adsorption of both thiophene and H_2S, deduced from both experiments and theory, has been reported in the literature. For example, Lee and Butt [24] have found a heat of adsorption for thiophene of -50 kJ/mol while Satterfield and Roberts [22] report of a value of about -75–-100 kJ/mol. Furthermore, while the first authors found a higher heat of adsorption for H_2S than for thiophene, Satterfield and Roberts reported the opposite. Van Parijs and Froment [34] reported heats of adsorption of thiophene of -44.7 and -52.7 kJ/mol, respectively, depending on the kinetic model used to fit the experimental data. Theoretical values of the heat of adsorption of thiophene vary between -62 and -137 kJ/mol, whereas the values for the heat of adsorption of H_2S vary between -75 and -93 kJ/mol [10]. Recently, Rodriguez et al. [35] reported on the adsorption of thiophene on unpromoted and Ni-promoted molybdenum sulfide. They estimated that the adsorption energy of thiophene on a MoS_x system is about -63 kJ/mol while on Ni-promoted MoS_x is between -84 and -105 kJ/mol. For a MoS_x system, they also reported that few thiophene molecules remain on the surface at 250 K and thiophene is fully removed at 300 K. According Tarbuck et al. [36], thiophene desorbs in a single peak with a maximum at 240 K on MoS_x/Al_2O_3 catalysts. This might indicate a lower adsorption energy on supported catalysts, which is in better agreement with the heat of adsorption of thiophene reported in this contribution for supported NiMo planar model catalysts.

5. Conclusions

In this contribution we have determined intrinsic kinetic parameters for the relatively simple thiophene hydrodesulfurization test reaction on planar nonporous model catalysts. Kinetic experiments on a NiMo planar model catalyst, performed over a temperature range 573–673 K, allow for the estimation of the activation energy, $E_{\text{act}}^{\text{rds}} \approx 85$ kJ/mol, and the heats of adsorption of thiophene and H_2S, $-\Delta H_{\text{ads}}^{\text{thioph}} \approx 60$ kJ/mol and $-\Delta H_{\text{ads}}^{\text{H}_2\text{S}} \approx 120$ kJ/mol. These values were obtained over well-defined model catalysts in a broad temperature range and under diffusion-free limitations. We emphasize that to the best of our knowledge these are the first kinetic experiments performed on a square centimeter model of an industrial catalyst. This work demonstrates how measuring intrinsic kinetics on planar surface science models can become an important tool for unraveling the mechanisms of catalytic reactions. Therefore, planar model catalysts offer

an excellent opportunity to study reaction mechanism and kinetics without diffusion limitations.

Acknowledgments

This research was conducted under the auspices of NIOK, The Netherlands Institute for Catalysis Research, with financial support from the Chemical Science Division of the Netherlands Organization for Scientific Research (NWO-CW) and the Netherlands Technology Foundation (STW). A.B. is especially indebted to NWO-CW for a visitor grant.

References

[1] R. Prins, V.H.J. de Beer, G.A. Somorjai, Catal. Rev. Sci. Eng. 31 (1989) 1.
[2] H. Topsøe, B.S. Clausen, F.E. Massoth, Hydrotreating Catalysis, Springer, Berlin, 1996.
[3] S. Eijsbouts, Appl. Catal. A 158 (1997) 53.
[4] S. Kolboe, Can. J. Chem. 47 (1969) 352.
[5] J.M.J.G. Lipsch, G.C.A. Schuit, J. Catal. 15 (1969) 179.
[6] E.J.M. Hensen, M.J. Vissenberg, V.H.J. de Beer, J.A.R. van Veen, R.A. van Santen, J. Catal. 163 (1996) 429.
[7] J.K. Nørskov, B.S. Clausen, H. Topsøe, Catal. Lett. 13 (1992) 1.
[8] H. Topsøe, B.S. Clausen, N.Y. Topsøe, J. Hyldtoft, J.K. Nørskov, Am. Chem. Soc., Div. Petrol. Chem. 38 (1993) 638.
[9] S. Kasztelan, Appl. Catal. A 83 (1992) L1.
[10] M. Neurock, R.A. van Santen, J. Am. Chem. Soc. 116 (1994) 4427.
[11] H. Toulhoat, P. Raybaud, S. Kasztelan, G. Kresse, J. Hafner, Catal. Today 50 (1999) 629.
[12] E.J.M. Hensen, V.H.J. de Beer, R.A. van Santen, T. Weber, in: R. Prins, R.A. van Santen (Eds.), Transition Metal Sulphides: Chemistry and Catalysis, Kluwer, Dordrecht, 1998, p. 169.
[13] P.L.J. Gunter, J.W. Niemantsverdriet, F.H. Ribeiro, G.A. Somorjai, Catal. Rev. Sci. Eng. 39 (1997) 77.
[14] L. Coulier, V.H.J. de Beer, J.A.R. van Veen, J.W. Niemantsverdriet, Top. Catal. 13 (2000) 99.
[15] G. Kishan, L. Coulier, V.H.J. de Beer, J.A.R. van Veen, J.W. Niemantsverdriet, J. Catal. 196 (2000) 180.
[16] L. Coulier, V.H.J. de Beer, J.A.R. van Veen, J.W. Niemantsverdriet, J. Catal. 197 (2001) 26.
[17] G. Kishan, L. Coulier, J.A.R. van Veen, J.W. Niemantsverdriet, J. Catal. 200 (2001) 194.
[18] A. Borgna, E.J.M. Hensen, L. Coulier, M.H.J.M. de Croon, J.C. Schouten, J.A.R. van Veen, J.W. Niemantsverdriet, Catal. Lett., in press.
[19] E.J.M. Hensen, H.J.A. Brans, G.M.H.J. Lardinois, V.H.J. de Beer, J.A.R. van Veen, R.A. van Santen, J. Catal. 192 (2000) 98.
[20] R.G. Leliveld, A.J. van Dillen, J.W. Geus, D.C. Koningsberger, J. Catal. 175 (1998) 108.
[21] F.E. Massoth, K.S. Chung, in: Proc., 7th ICC, Tokyo, 1980, p. 629.
[22] C.N. Satterfield, G.W. Roberts, AIChE J. 14 (1968) 159.
[23] F.E. Massoth, J. Catal. 47 (1977) 316.
[24] H.C. Lee, J.B. Butt, J. Catal. 49 (1977) 320.
[25] M.L. Vrinat, Appl. Catal. 6 (1983) 137.
[26] M.J. Girgis, B. C Gates, Ind. Eng. Chem. Res. 30 (1991) 2021.
[27] D. Sullivan, J. Ekerdt, J. Catal. 178 (1998) 226.
[28] J. Leglise, L. Finot, J. van Gestel, J.C. Duchet, Stud. Surf. Sci. Catal. 127 (1999) 51.
[29] A.N. Startsev, J. Mol. Catal. A 152 (2000) 1.
[30] R. Shafi, G.J. Hutchings, Catal. Today 50 (2000) 423.
[31] S. Ihm, S. Moon, H. Choi, Ind. Eng. Chem. Res. 29 (1990) 1147.
[32] M.J. Ledoux, O. Michaux, G. Agostine, J. Catal. 102 (1986) 275.
[33] J. Leglise, J. van Gestel, J.C. Duchet, in: Symp. Adv. Hydrotreating Catalysts, vol. 533, ACS, Washington, DC, 1994.
[34] I.A. van Parijs, G.F. Froment, Ind. Eng. Chem. Prod. Res. Dev. 25 (1986) 437.
[35] J.A. Rodriguez, J. Dvorak, A.T. Capitano, A.M. Gabelnick, J.L. Gland, Surf. Sci. Lett. 429 (1999) L462.
[36] T.L. Tarbuck, K.R. McCrea, J. W Logan, J.L. Heiser, M.E. Bussell, J. Phys. Chem. B 102 (1998) 7845.